

# A study of slipstreams in triple shock wave configurations

L. Gvozdeva<sup>1</sup> · S. Gavrenkov<sup>1</sup> · A. Nesterov<sup>1</sup>

Received: 17 November 2013 / Revised: 22 February 2015 / Accepted: 10 March 2015 / Published online: 3 April 2015  
© Springer-Verlag Berlin Heidelberg 2015

**Abstract** A shock wave appearing in supersonic gas flow reflects in different ways depending on flow conditions. It can take the form of regular or irregular reflection. For the irregular reflection configuration of three shock waves and a slipstream arises. Mathematical investigations of the development of parameters across slipstream in triple shock configuration have been made with variation of the angle of incidence of the shock wave, the shock wave Mach number and the adiabatic index of the gas. It has been shown that the characteristic mixing parameters of the slipstream increase with the increase of Mach number of the flow and the decrease of the heat capacity ratio. This leads to an increase of vortex formation and an increase of the angular spread of the slipstream. It also has been shown that the angle between the reflected wave and the slipstream diminishes with the decrease in heat capacity ratio so that the value may become of the same order as the spread angle. This may lead to quantitative changes in the whole reflection pattern near the triple point. The evident dependence of slipstream instability magnitude on the physical and chemical transformation intensity in the fluid was previously experimentally observed. The results of an analytical investigation appeared to be in good agreement with the experimental data.

Communicated by G. Ciccarelli.

This paper is based on work that was presented at the 24th International Colloquium on the Dynamics of Explosions and Reactive Systems, Taipei, Taiwan, July 28–August 2, 2013.

✉ L. Gvozdeva  
gvozdevalg@mail.ru

<sup>1</sup> Joint Institute for High Temperatures of the Russian Academy of Sciences (JIHT RAS) 125412, Izhorskaya st. 13 Bd. 2, Moscow, Russia

**Keywords** Shock wave reflection · Triple shock configuration · Slipstream · Adiabatic index · Kelvin–Helmholtz instability

## List of symbols

$M_0$	Mach number of incident shock wave
$M_1$	Mach number of gas flow
$a$	Speed of sound
$u$	Normal component of gas velocity relative to the shock wave
$V$	Absolute velocity of gas flow
$P$	Pressure
$T$	Temperature
$h$	Enthalpy
$\rho$	Density
$R$	Universal gas constant
$\mu$	Molecular weight
$\gamma$	Adiabatic index or ratio of specific heats
$\chi$	Angle between triple point path and the wedge surface
$\alpha_0$	Wedge angle
$\omega_1$	Incidence wave angle
$\omega_2$	Reflected wave angle
$\phi$	Inclination angle
$\omega_{RT}$	Angle between reflected wave and the slipstream
$\delta$	Slipstream spread angle

## 1 Introduction

Two forms of reflection are well known in a steady supersonic stream of gas: the two-shock (regular reflection, Fig. 1) and the three shock wave configuration (irregular or Mach

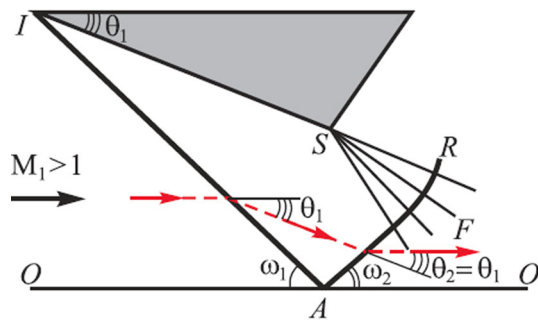


**Fig. 1** Regular reflection.  $IA$  incident wave,  $AR$  reflected wave,  $OO$  reflection line,  $M_1$  Mach number of flow,  $\omega_1$  incident wave angle,  $\omega_2$  reflected wave angle,  $\theta_1$  deflection angle after incident shock wave and angle of the wedge,  $\theta_2$  flow deflection angle after reflected wave,  $A$  point of intersection,  $SF$  rarefaction fan

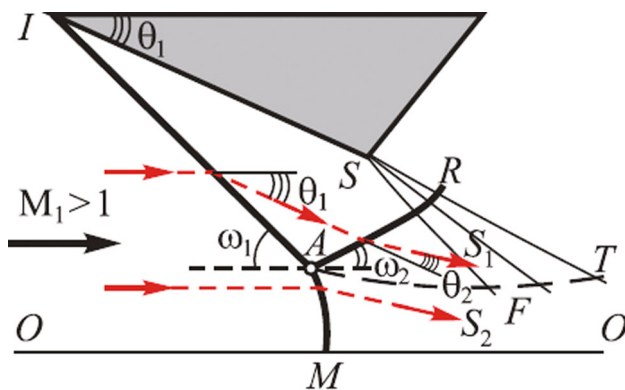


**Fig. 2** Mach reflection with positive reflection angle.  $\omega_2 > 0$ ,  $A$  triple point,  $AM$  Mach stem

reflection, Fig. 2). In the second case, the section  $AM$  of the configuration is called the Mach stem;  $AR$  is the reflected wave;  $AI$  is the incident wave and  $AT$  is the slipstream separating the gas passing through the incident wave  $AI$  and the reflected wave  $AR$  ( $S_1$  in Fig. 2) and the gas passing through the Mach stem  $AM$  ( $S_2$  in Fig. 2) [3–5, 11, 16, 25].

Slipstreams are unstable; they collapse into a chain of vortices due to the Kelvin–Helmholtz instability (K.-H.). The K.-H. instability occurs when two fluids flow in proximity to each other with a tangential velocity difference (Fig. 3). This type of instability occurs in a triple shock configuration. The Kelvin–Helmholtz instability is of fundamental interest [1]. It is of high importance in fields such as turbulence, small-scale mixing in the Richtmyer–Meshkov and the Rayleigh–Taylor instabilities. An understanding of the stability characteristics of compressible mixing layers is also important in view of the use of the scramjet engine for the propulsion of hypersonic aircraft.

Determining the gas parameters and triple shock configuration angles usually is done with the aid of the three-shock theory. For a perfect gas in the two-dimensional case, the flow pattern is determined from the inflowing Mach num-

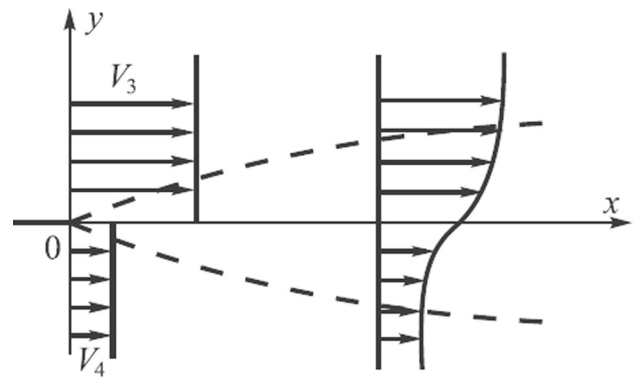


**Fig. 3** Initial velocity profiles at the triple point and downstream in the slipstream

ber,  $M_1$ , angle of incidence,  $\omega_1$ , and the adiabatic index,  $\gamma$ , only [3–5, 16, 18, 25]. Behind strong shock waves different physical and chemical reactions occur: vibration excitation, dissociation, ionization etc. In [27] it was shown that these processes could be taken into account by considering the adiabatic index. The evolution of the slipstream in the triple shock wave configuration in the unsteady reflection case was first observed in shock tube experiments [2–5, 8, 21, 22, 24]. The development of flow instabilities and transition to turbulence have been studied theoretically and numerically [20] on the basis of results given in [6, 14, 19] for the quasi-steady case, and in [15, 17] for the steady case.

Despite the fact that there are many papers considering the development of the mixing layer instability, the problem of dependence of mixing on the adiabatic index has not been investigated properly. Most numerical research was done with  $\gamma = 1.4$  to compare with wind tunnel experiments [12]. In shock tube experiments with strong shock waves, however, one can see that there is a strong dependence on adiabatic index.

Moreover, as has become recently known, the location of the shock waves in the three shock configuration is very sensitive to the value of the adiabatic index. With the decrease of the adiabatic index to  $< 1.4$  and the increase of  $M_1$  to more than 3, a new form of the Mach reflection with a negative reflected wave angle appears as a solution to the equations of three-shock theory [7, 9, 10]. It has been shown that this form of reflection in steady flow would be unstable when it appears at the transition from regular reflection. Such a form of unstable double Mach reflection in steady flow is shown in Fig. 4. One should note that it has been universally acknowledged that the different forms of double Mach reflection can exist only in unsteady or quasi-steady reflection [5]. Thus, the investigation of the dependence of the reflection angle on adiabatic index has led to fundamentally new results.

The aim of this work is to determine how the change in the adiabatic index affects the development of the Kelvin–Helmholtz instability of the slipstream in the triple shock

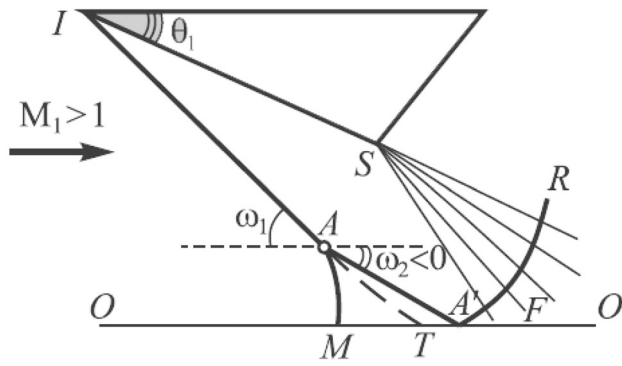


**Fig. 4** Mach reflection with negative reflection angle. *A* the first triple point, *A'* the second triple point.  $\omega_2 < 0$

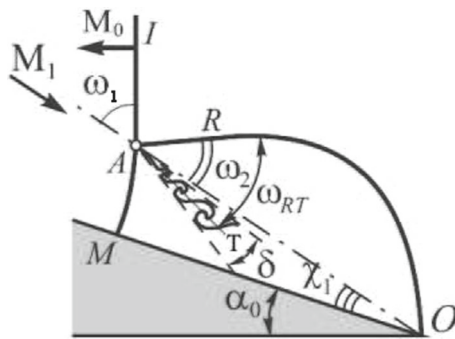


**Fig. 5** Scheme of shock wave reflection off the wedge with the angle  $\alpha_0$ . *IA* incident wave, *AR* reflected wave, *AM* Mach wave, *AT* slipstream,  $M_0$  Mach number of incident wave,  $M_1$  Mach number of the flow in the system of reference connected with the triple point,  $\omega_1$  the angle between incident wave and the trajectory of the moving of the triple point,  $\omega_2$  the angle between reflected wave and the trajectory of the moving of the triple point;  $\delta$  the spread angle,  $\omega_{RT}$  the angle between the reflected wave and the slipstream,  $\chi_1$  the angle of the path of the first triple point

configuration. This has been done analytically with the aid of three-shock theory. Comparison with experimental data has been undertaken.

**2 Prior experiments in shock tubes**

Shock wave reflection configurations can be found in steady as well as in unsteady flows. Let a shock wave traveling at Mach number  $M_0$  hit a rigid surface at an angle  $\alpha_0$  (Fig. 5). The entire system is self-similar with a triple point *A* moving at a constant angle  $\chi_1$  to the wedge surface. From geometric consideration, it is seen that relative to the triple point *A*, the approaching gas has a Mach number  $M_1 = M_0/\sin(\omega_1)$ , where  $\omega_1 = 90 - \alpha_0 - \chi_1$ .

Several forms of quasi-stationary reflection of shock waves were found. The schemes are given in Fig. 6. Simple Mach reflection is seen in Fig. 6a. The contact surface is set along the wall of the wedge towards the vertex *O*.

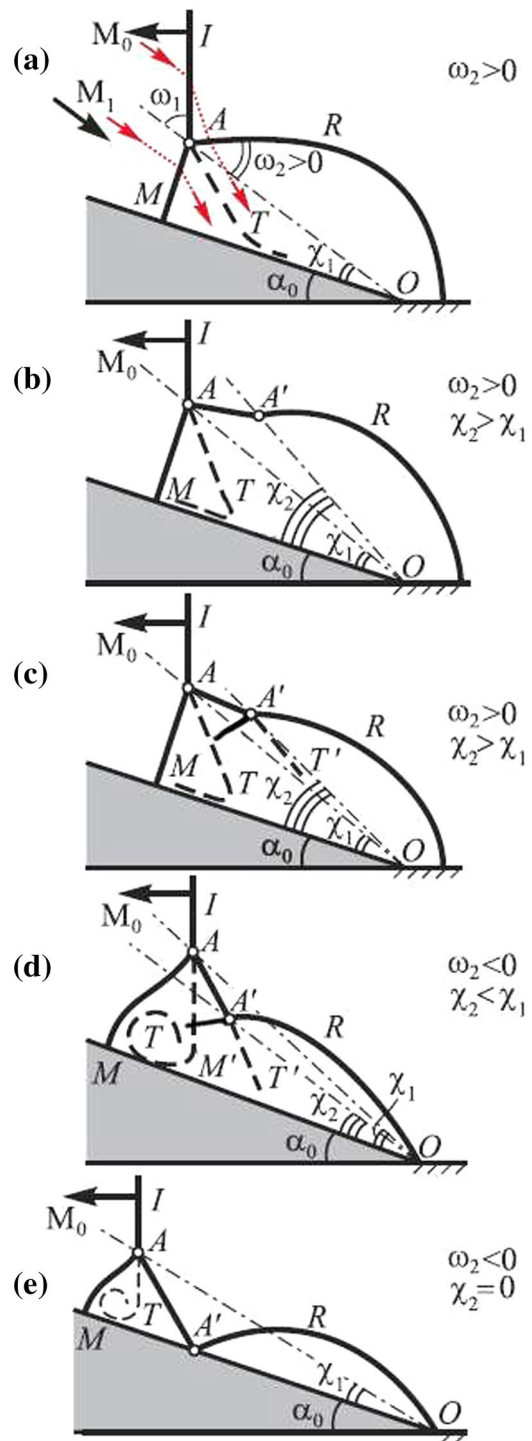


**Fig. 6** **a** single Mach reflection, **b** complex Mach reflection, **c** double Mach reflection with positive reflection angle, **d** double Mach reflection with negative reflection angle, **e** terminal double Mach reflection. *IA* incident shock wave, *AR* reflected wave, *AM* Mach stem, *AT* slipstream, *A* first triple point, *A'* second triple point,  $\chi_1$  angle of first triple point,  $\chi_2$  angle of second triple point

Experiments have shown that if the angle  $\alpha_0$  is further increased, the reflection may occur as a complex Mach reflection (Fig. 6b) which is characterized by a kink in point *A'*

in the reflected wave and the slipstream curling into a vortex. Further increase in  $\alpha_0$  results in double Mach reflection in which a second triple point  $A'$  is formed on the reflected wave, and a second shock wave  $AM'$  and a second slipstream  $A'T'$  are generated (Fig. 6c, d), or to the terminal form in which the second triple point  $A'$  moves along the wedge surface (Fig. 6e). The two forms of double Mach reflection in Fig. 6c, d differ in that the angle  $\omega_2 > 0$  (i.e.  $\chi_2 > \chi_1$ ) in Fig. 6c and the angle  $\omega_2 < 0$  (i.e.  $\chi_2 < \chi_1$ ) in Fig. 6d.

For the unsteady reflection the flow pattern is self-similar, i.e., the location of the waves depends only on the ratio  $x/t$ , where  $x$  is spatial coordinate,  $t$  is time. The triple point  $A$  is moving at a constant angle  $\chi_1$  to the surface. In the coordinate system associated with the triple point  $A$  (Fig. 5), the pattern of this system is steady, and we get a typical picture of the formation of the free mixing layer in the region behind the reflected wave. Thus, free mixing layers can be simulated by irregular reflection.

Let us look at the results of experiments made in shock tubes from the point of view of the adiabatic index influence on the mixing process. Simulation of mixing layers in shock tubes has the advantage that, unlike wind tunnels, one can use a gas with low values of the adiabatic index. The experiments were conducted in a shock tube of square cross-section in argon, air, nitrogen, carbon dioxide and Freon 12 [2,8,21–23]. Thus, the ratio of specific heats of the gas varied from  $\gamma = 1.66$  down to  $\gamma = 1.18$ . The change of the specific heat leads to the change in gas compressibility and velocity of sound. Some of the experimental results are shown in Fig. 7.

We see simple Mach reflection in Fig. 7a in nitrogen (like the form shown in Fig. 6a). At a Mach number of the incident shock wave  $M_0 = 2.12$  nitrogen behaves as an ideal gas with  $\gamma = 1.4$ . The same is true for air in Fig. 7b. We see in these pictures that the slipstream collapses into a chain of vortices. In Fig. 7b, the slipstream collapses near the wall into a big vortex. This is due to the increase in the pressure at the wall to the right of the contact surface.

The behavior of the slipstream near the wall (Fig. 6c) is determined by the whole picture of the flow. The so-called wall-jetting effect is explained in [3–5,11,24] and investigated in detail numerically in [26]. Certainly, in this case the modeling of the mixing is possible only in the vicinity of the triple point where the pressure of both sides of a slipstream is the same. On the wedge surface, in the case of the complex form of Mach reflection (Fig. 6b), the pressure to the right of the slipstream is higher than that to the left. This case of reflection is presented in Fig. 7b—Mach reflection with the inflection on the reflected wave.

In Fig. 7a, b the spread angle  $\delta$  of the contact surface is about  $4^\circ$ . In Fig. 7c, d one can see a notable increase of the spread angle  $\delta$ . It is  $24^\circ$  in Fig. 7c and about  $27^\circ$  in Fig. 7d. In these cases, with certain Mach numbers behind the shock waves, the following chemical and physical processes occur:

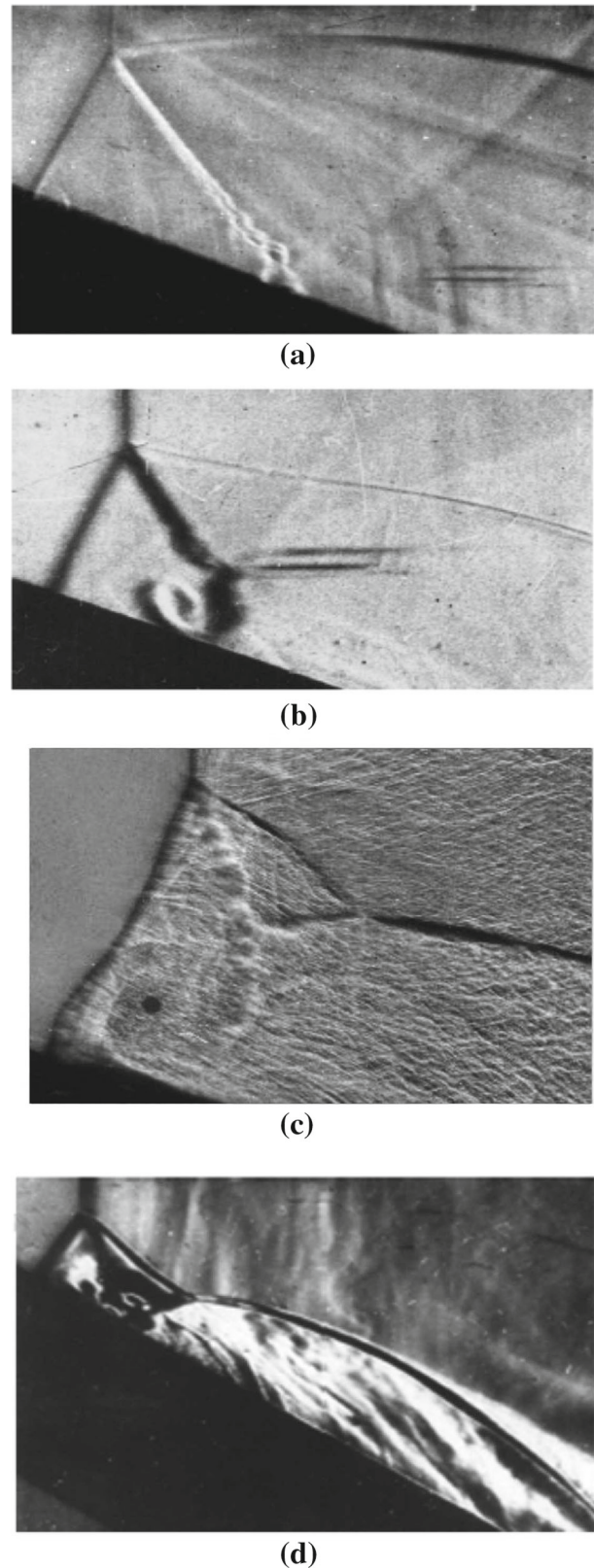


**Fig. 7** Schlieren pictures of shock wave reflection from a wedge: **a** in nitrogen,  $\alpha_0 = 24^\circ$ ,  $M_0 = 2.12$ ,  $P_0 = 50$  Torr [2]; **b** in air,  $\alpha_0 = 24^\circ$ ,  $M_0 = 3.55$ ,  $P_0 = 12.7$  Torr [2]; **c** in Fr-12,  $\alpha_0 = 15^\circ$ ,  $M_0 = 3.84$  [23]; **d** in carbon dioxide gas,  $\alpha_0 = 32^\circ$ ,  $M_0 = 5.18$ ,  $P_0 = 20$  Torr [8]



vibration, excitation and dissociation, so that the adiabatic index decreases to  $\gamma = 1.2$  in  $\text{CO}_2$  and  $\gamma = 1.16$  in Fr-12. The reflection configuration in Fig. 7b corresponds to the pattern with the inflection on the reflected wave (Fig. 6b), and the  $\text{CO}_2$  (the carbon dioxide) reflection configuration in Fig. 7d is the double Mach reflection with the negative reflection angle (Fig. 6d). One can see the second triple point and secondary Mach stem connected with the second triple point. Thus, the experiments held in the shock tubes clearly show that physical–chemical transformations have a strong influence on the mixing of the slipstream.

### 3 Analytical calculation of triple shock configuration

For determining the parameters at the mixing layer the three-shock theory is used with the shock polar method [18]. This theory can be used if in the vicinity of the triple point all three waves are straight, because it is known that the calculations are in good agreement with experiment when the flow behind the reflected wave is supersonic in the system of reference connected with the triple point [4,5]. For given initial parameters of the gas and the intensity of the shock wave, all gas parameters can be calculated on the boundary of the mixing region.

Consider the vicinity of the triple point A (Fig. 8a): suppose a supersonic flow with Mach number  $M_1$  flows into the shock wave IA at the angle  $\omega_1$ . For incident, reflected and Mach stem shock wave, the conservation laws give the relations:

$$\begin{aligned} \rho_i u_i &= \rho_j u_j & (1) \\ \rho_i u_i^2 + P_i &= \rho_j u_j^2 + P_j & (2) \\ \frac{u_i^2}{2} + h_i &= \frac{u_j^2}{2} + h_j & (3) \\ \mu &= f(P, T) & (4) \\ h &= f(P, T) & (5) \end{aligned}$$

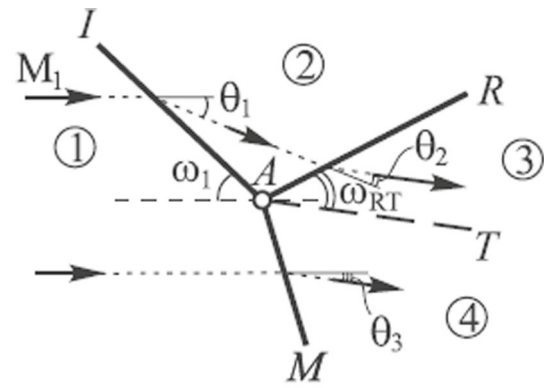
where  $\rho$  density,  $u$  velocity normal to the shock wave,  $P$  pressure,  $\mu$  molecular weight,  $h$  enthalpy,  $R$  universal gas constant. The subscript  $i$  is used for the region before the shock wave, and  $j$  for the region behind the shock wave.

The deflection angle  $\theta$  should satisfy the following dependence from geometrical consideration:

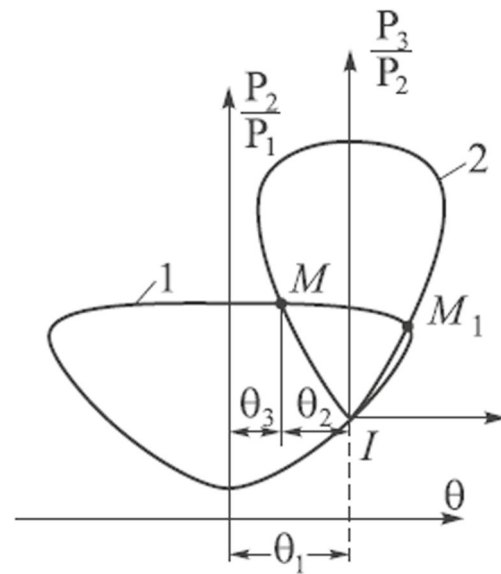
$$\frac{\tan(\phi_i - \theta_i)}{\tan(\phi_i)} = \frac{\rho_i}{\rho_j} \tag{6}$$

or

$$\theta_1 = \arctan \left( \frac{1 - \frac{\rho_i}{\rho_j} \tan(\phi_i)}{1 + \frac{\rho_i}{\rho_j} \tan(\phi_i)} \right) \tag{7}$$



(a)



(b)

**Fig. 8** Three shock wave configuration in the coordinate system associated with the triple point (a), shock polars (b)

where  $\phi$  is the inclination angle and  $\theta$  is the angle of flow deflection.

For each Mach number  $M_1$  and the initial parameters  $P_i, \rho_i, T_i, h_i, \phi_i, \theta_i$  the solution of this system gives a curve—the shock polar in the plane  $\left(\frac{P_j}{P_i} - \theta_i\right)$  (curve 1 in Fig. 8 b). If moreover the angle  $\phi_1 = \omega_1$  is known, then the initial state is represented by a point  $I$  on the polar.  $M_i = \frac{V_i}{a_i}$ , where  $V_i = \frac{u_i}{\sin(\phi_i)}$  is the velocity of the gas flow, and  $a_i$  is the speed of sound.

The intersection of the polar for the Mach stem wave and the polar for the reflected wave will solve the problem of irregular reflection, as it has fulfilled the condition of compatibility:

$$P_3 = P_4 \tag{8}$$

$$\theta_3 = \theta_1 - \theta_2 \tag{9}$$

The intersection occurs at points  $M$  and  $M_1$  (Fig. 8 b). The solution is point  $M$ , and the analysis of experimental data shows that the Mach wave should be a strong wave. The angle between the reflected wave and slipstream in the configuration can be found from the relations:

$$\omega_{RT} = \omega_2 + \theta_3 \quad (10)$$

$$\omega_2 = \phi_2 - \theta_1 \quad (11)$$

where  $\omega_2$  is the angle between the reflected wave and the direction of the inflow to the reflected wave. Thus, using this technique, we can determine all parameters of the flow at the slipstream, the location of the shock waves and the slipstream in dependence on Mach number  $M_1$ , incidence angle  $\omega_1$ , and the initial parameters of a gas  $P_1, T_1$ .

This system of equations is valid in the common case when physical-chemical transformations occur in the gas behind the shock wave with the only requirement being thermodynamic equilibrium with constant temperature and pressure. But the solution of such a system is a lot more complicated and can only be done numerically since the functions  $\mu(T, \rho)$  and  $h(T, \rho)$  for the gas should be known. Therefore, the solution for the triple shock in gases with physical-chemical transformations is obtained only in some special cases mentioned in monographs [3–5]

However, to obtain the general solution for an ideal gas, it was assumed that the molecular weight is constant and the enthalpy depends on the adiabatic index as follows:

$$h = \frac{\gamma}{\gamma - 1} \frac{p}{\rho} \quad (12)$$

Thus, the equations transform to a system which can be solved easily. The solution in this case depends on the Mach number  $M_1$ , incidence angle  $\omega_1$  and adiabatic index  $\gamma$ . This is the way calculations are typically performed with a constant adiabatic index of 1.4 and 1.66 [11, 12, 16, 25].

#### 4 Results and discussions. Dependence of gas parameters on adiabatic index

In this paper, the dependence of governing dimensional parameters at the slipstream on the adiabatic index has been examined. In addition,  $\omega_{RT}$ , the angle between the reflected wave AR and the slipstream AT, has been determined.

The whole system of equations has been written in terms of the parameters pressure  $P_1$ , temperature  $T_1$ , the incidence angle  $\omega_1$ , the Mach number  $M_1$  and the value of the adiabatic index  $\gamma$ . The basic dimensionless parameters of the gas mixture at the slipstream AT and the angle  $\omega_{RT}$  have been calculated as a function of the adiabatic index. The calculations were made for the value of the adiabatic index  $\gamma$  in the

range from 1.01 to 1.66. The Mach number of the incoming flow  $M_1$  in the coordinate system associated with the triple point varies from 3 to 15, and the initial temperature is  $T_1 = 293$  K. The results are presented in Fig. 9 for the constant angle  $\omega_1 = 40^\circ$ .

It is seen that in the range of investigated values of  $\gamma$ , the parameters temperature ratio, density, speed of sound, Mach number vary significantly with decreasing value of the adiabatic index (Fig. 9a–d). As to the velocity ratio (Fig. 9e)—the main governing parameter for the flow mixing [1]—it can be seen that for any Mach number  $M_1$ , the  $\gamma$  reduction leads to an increase in velocity ratio. The influence of the adiabatic index  $\gamma$  is stronger with the greater values of  $M_1$ . Dependence of the angle  $\omega_{RT}$  on the adiabatic index is also indicated (Fig. 9f). Note that in this case the decrease of the adiabatic index for any Mach number leads to a very noticeable decrease in the angle between the reflected wave and the contact surface. This angle is reduced by 2 or 3 times, even for low Mach numbers. The results, as it is seen, show the need to consider the value of adiabatic index when calculating compressible slipstream flows, since it varies significantly due to the physical-chemical transformation.

As it has been discussed in the introduction, there are not many papers in which the development of the Kelvin–Helmholtz instability for the unsteady case is treated theoretically [14, 19, 20]. There are different theories suggested for the description of mixing process. It is possible to verify some proposed criteria using the results of the calculation presented. Future investigation will be aimed at the theoretical determination of the spread angle of the slipstream in triple shock configuration in dependence on  $M_1, \omega_1$  and  $\gamma$ .

#### 5 Comparison with experiments

In order to compare the calculations with experiments, new processing of the experimental data has been done (Figs. 10, 11). The experiments were performed for the quasi-stationary case for shock waves reflected off the corner with the angle  $\alpha_0$ . In applying the formulas for the steady case, one should use the system of reference connected with the triple point. So, for correct processing of experiments one should know the angle  $\chi_1$ , the angle of the path of triple point. This angle is known only for the photos of Fig. 7b, d. When the angle  $\chi_1$  can be determined, the angle of incidence  $\omega_1$  found from the relation  $\omega_1 = 90^\circ - \chi_1 - \alpha_0$ . The Mach number of the incoming flow can be determined from the relation  $M_1 = \frac{M_0}{\sin(\omega_1)}$ .

In the general case of strong shock waves, when physical-chemical reactions occur behind the shock wave, the self-similarity assumption does not hold true because of relaxation effects. However, in cases where either part equilibrium

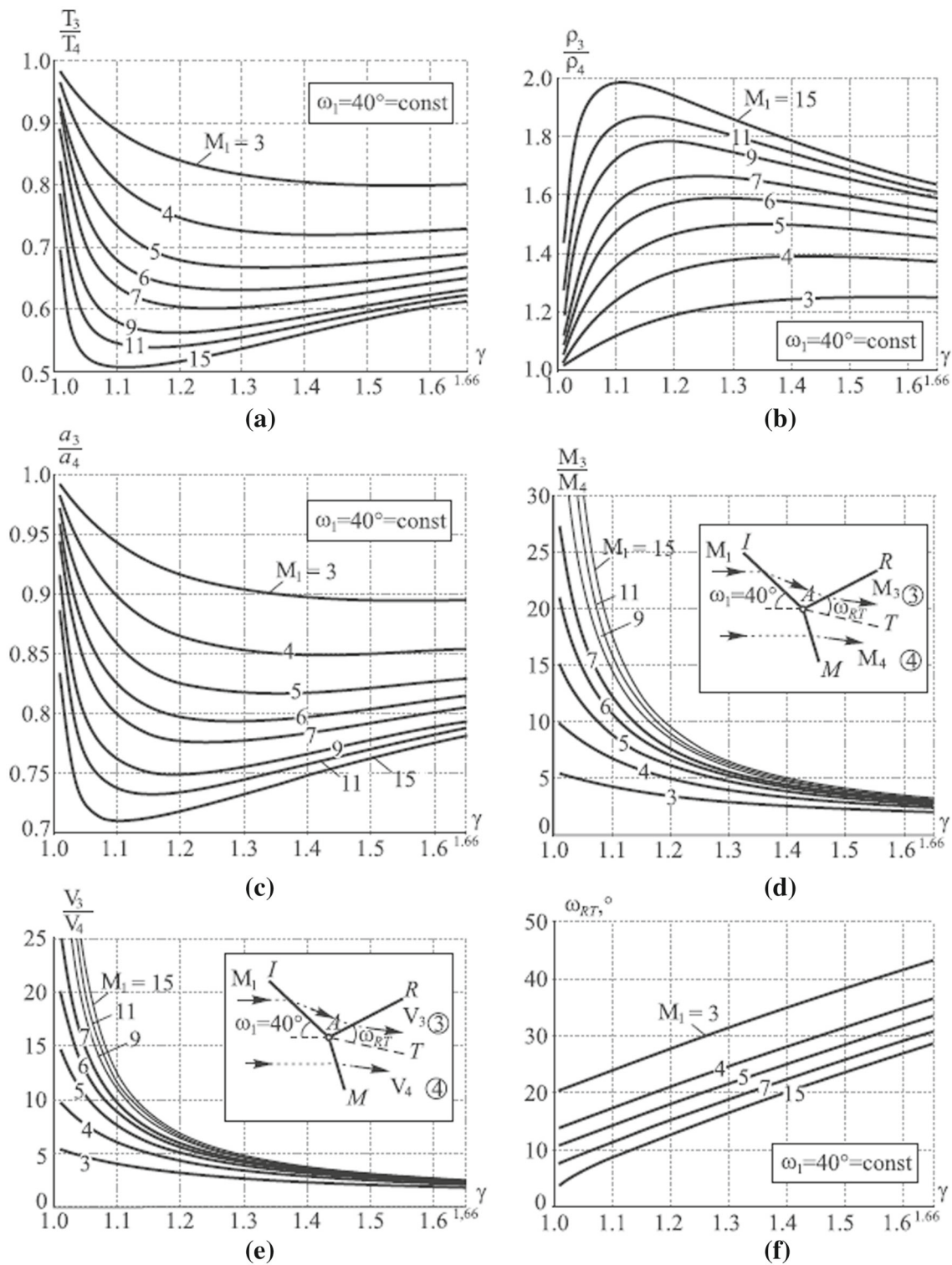


**Fig. 9** Dependence of the parameters at the slipstream, on the adiabatic index  $\gamma$  for different Mach numbers  $M_1$ . The angle of incidence is  $\omega_1 = 40^\circ = \text{const}$  **a**  $T_3/T_4$ ; **b**  $\rho_3/\rho_4$ ; **c**  $a_3/a_4$ ; **d**  $M_3/M_4$ ; **e**  $V_3/V_4$ ; angle  $\omega_{RT}$  between the reflected wave AR and tangential surface AT

or complete thermodynamic equilibrium becomes established behind the shock, self-similar solutions are, in fact, possible.

In air (Fig. 7b) there are no physical-chemical transformations, so we can use  $\gamma = 1.4$ . The detailed investigation of the thermodynamical state of carbon dioxide in different

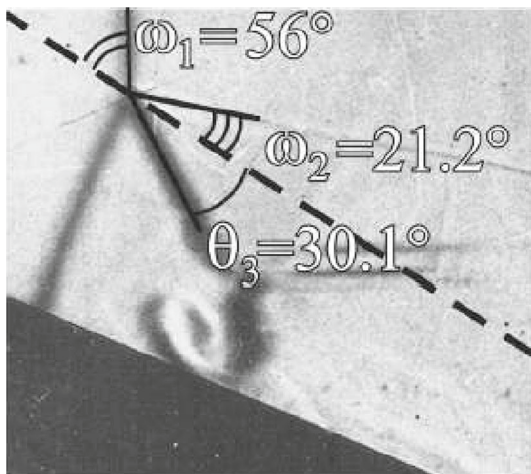


**Fig. 10** Enlarged photo of Fig. 7b, reflection in air. The shock wave configuration moves from right to left in the absolute frame of reference.  $\alpha_0 = 24^\circ$ ,  $M_0 = 3.55$ ,  $P_1 = 12.7$  Torr. The dashed line indicates the path of the triple point

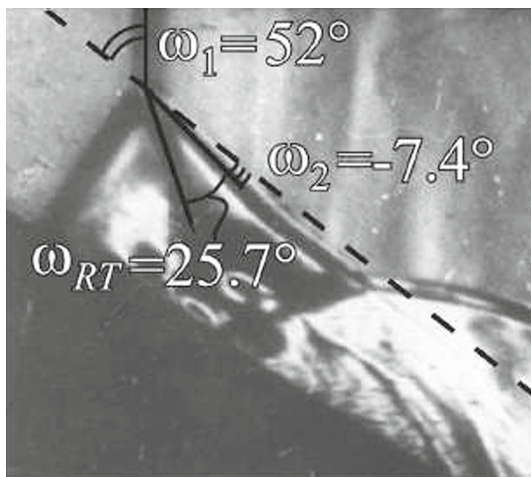


**Fig. 11** Enlarged photo of 7d, reflection in carbon dioxide. The shock wave configuration moves from right to left in the absolute frame of reference.  $\alpha_0 = 32^\circ$ ,  $M_0 = 5.18$ ,  $P_1 = 20$  Torr. The dashed line indicates the path of the triple point

triple shock configurations is given in [2–4]. If we consider carbon dioxide as an ideal gas, one has to take the adiabatic index as 1.4 because the molecule of carbon dioxide is linear. But the excitation of molecules occurs even at room temperature and certainly behind the incident and reflected waves. In addition, at the temperatures behind the incident wave, carbon dioxide must dissociate. It was stated, that in the above experiment, the relaxation times for the processes of vibration excitation and dissociation are very different. Dissociation will affect the flow not earlier than 100  $\mu\text{s}$  after the passage of the shock wave. Vibration excitation occurs faster, in  $<10$   $\mu\text{s}$ . Thus, one can use the assumption about part thermodynamic equilibrium [2]. The value of the adiabatic index equals to 1.2 in all areas for the experiment in Fig. 7d was found using the Ivtanthermo database [13].

**Table 1** Results of processing of the experiment in Fig. 7b for  $\gamma = 1.4$ ,  $M_1 = 4.28$ ,  $\omega_1 = 56^\circ$

$i$	$T_i$ (K)	$P_i$ ( $P_a$ )	$p_i$ ( $\text{kg/m}^3$ )	$M_i$	$V_i$ (m/s)	$a_i$ (m/s)
3	1093	$34 \times 10^4$	0.11	1.12	742	666
4	1285	$34 \times 10^4$	0.094	0.57	409	721
3/4	0.85	1	1.17	1.97	1.81	0.92

**Table 2** Comparison between the experiment and calculations in Fig. 7b for  $\gamma = 1.4$ ,  $M_1 = 4.28$ ,  $\omega_1 = 56^\circ$

	$\omega_1$ ( $^\circ$ )	$\omega_2$ ( $^\circ$ )	$\theta_3$ ( $^\circ$ )	$\omega_{RT}$ ( $\omega_2 + \theta_3$ )
Calc.	56	21.2	30.1	51.3
Exp.	56	20	30	50

**Table 3** Processing of the experiment in Fig. 7d for  $\gamma = 1.2$  and 1.4,  $M_1 = 6.57$ ,  $\omega_1 = 52^\circ$ ,  $\text{CO}_2$

	$\gamma = 1.4$	$\gamma = 1.2$	Exp.
$V_3/V_4$	2.39	3.97	–
$\omega_{RT}$ ( $^\circ$ )	37.5	25.7	24

**Table 4** Processing of the experiment in Fig. 7d for  $\gamma = 1.2$ ,  $M_1 = 6.57$ ,  $\omega_1 = 52^\circ$ ,  $\text{CO}_2$

$i$	$T_i$ (K)	$P_i$ ( $P_a$ )	$p_i$ ( $\text{kg/m}^3$ )	$M_i$	$V_i$ (m/s)	$a_i$ (m/s)
3	1156	$12.5 \times 10^4$	0.57	1.87	956	512
4	1533	$12.5 \times 10^4$	0.43	0.41	241	589
3/4	0.75	1	1.33	14.56	3.97	0.87

**Table 5** Comparison between the experiment and calculations in Fig. 7d for  $\gamma = 1.2$ ,  $M_1 = 6.57$ ,  $\omega_1 = 52^\circ$ ,  $\text{CO}_2$

	$\omega_1$ ( $^\circ$ )	$\omega_2$ ( $^\circ$ )	$\theta_3$ ( $^\circ$ )	$\omega_{RT}$ ( $\omega_2 + \theta_3$ )
Calc.	52	–7.4	33.1	25.7
Exp.	52	–8	32	24

The results of the calculations of the experiment in Fig. 7b are given in Tables 1, 2 and in Fig. 10. As we can see from Table 2 and Fig. 10, there is a perfect consistency between experimentally measured and determined angles in the triple shock configuration.

The results of the calculation of the experiment in Fig. 7d are presented in Tables 3, 4, 5 and in Fig. 11. Two cases are given: ideal gas and vibration excitation with no dissociation. Table 3 shows that the excitation of molecules greatly affects the flow parameters. Parameter  $V_3/V_4$  for an adiabatic index of 1.2 is 1.66 times greater than for the ideal gas with  $\gamma = 1.4$ . The angle  $\omega_{RT}$  is approximately 11.8 $^\circ$  less than for the ideal gas. It coincides very well with the experimental data. Most pronounced is the increase of the spread angle of the slipstream due to the physical-chemical reaction behind the reflected wave. In the future it is intended to make theoretical



calculations of the spread angle in an extended range of initial parameters and compare the results with the experimental data.

## 6 Conclusions

The dependence of the basic parameters on the mixing of the slipstreams at the shock wave configuration has been determined as a function of the adiabatic index, Mach number and angle of incidence. It has been found that the slipstreams are greatly influenced by the physical and chemical transformations behind the shock wave which lead to the change in the adiabatic index of the gas. These conclusions are confirmed by the processing of experimental data conducted previously in shock tubes.

The increase in Mach number and the decrease of the adiabatic index lead to a significant decrease in the value of the angle between the slipstream and the reflected wave. The angle might become of the same order as the spread angle of the slipstream. In the case of quasi-steady reflection this should lead to the loss of self-similarity. In the steady case it should have strong influence on the interaction between vortices across the slipstream and the reflected wave and might lead to an instability in the flow structure near the triple point, especially in the case of triple shock configurations with negative reflection angle.

The increase of the Mach number and the decrease of the adiabatic index lead to a greater instability of the slipstream, so the mixing process is much more efficient in gases with a low adiabatic index. The study of the behavior of the slipstream is important from the point of view of the formation of turbulence behind unsteady shock waves, and therefore it may influence the deflagration to detonation transition (DDT) in tubes. The data obtained on turbulent mixing are of great importance in achieving advancement in laser-driven inertial confinement fusion (ICF).

**Acknowledgments** The present study is supported in part by the Russian Research Foundation for the Fundamental Sciences Grant 12-01-31362 and 14-08-01070. The authors gratefully thank Prof. Beric Skews for his insightful help in preparing this paper. Thanks are also due to the reviewers for their astute and helpful comments.

## References

1. Batchelor, G.K.: An Introduction to Fluid Dynamics. Cambridge University Press, Cambridge. ISBN:0521663962 (1970)
2. Bazhenova, T.V., Gvozdeva, L.G., Lobastov, Y.S., Naboko, I.M., Nemkov, R.G., Predvoditeleva, O.A.: Shock waves in real gases. English translation NASA TTS-585, Washington D.C. (1969)
3. Bazhenova, T.V., Gvozdeva, L.G.: Unsteady Intersection of Shock Wave (in Russian). Nauka, Moscow (1977)
4. Bazhenova, T.V., Gvozdeva, L.G., Nettleton, M.A.: Unsteady interaction of shock waves. *Prog. Aerosp. Sci.* **21**(3), 249–331 (1984)
5. Ben-Dor, G.: Shock Wave Reflection Phenomena, 2nd edn. Springer, New York (2007)
6. Brown, G., Roshko, A.: On density effects and large structure in turbulent mixing layers. *J. Fluid Mech.* **64**(4), 775–816 (1974)
7. Gavrenkov, S.A., Gvozdeva, L.G.: Numerical investigation of the onset of instability of triple shock configurations in steady supersonic gas flows. *Tech. Phys. Lett.* **38**(6), 587–589 (2012)
8. Gvozdeva, L.G., Predvoditeleva, O.A.: Experimental investigation of Mach reflection and shock waves with velocities of 1000–3000 m/sec in carbon dioxide gas, nitrogen and air. *Sov. Phys. Dokl.* **10**(8), 694–697 (1965)
9. Gvozdeva, L.G., Gavrenkov, S.A.: Formation of triple shock configurations with negative reflection angle in steady flows. *Tech. Phys. Lett.* **38**(4), 372–374 (2012)
10. Gvozdeva, L.G., Gavrenkov, S.A.: Influence of the adiabatic index on switching between different types of shock wave reflection in a steady supersonic gas flow. *Tech. Phys.* **58**(8), 1238–1241 (2013)
11. Hornung, A.: Regular and Mach reflection of shock waves. *Ann. Rev. Fluid Mech.* **18**, 33–58 (1986)
12. Ivanov, I.E., Kryukov, I.A.: III International Scientific and Technical Conference Aeroengines of XXI century. Moscow (2010)
13. Ivntanthermo database. [www.chem.msu.ru/rus/handbook/ivntan/welcome.html](http://www.chem.msu.ru/rus/handbook/ivntan/welcome.html) (In Russian)
14. Jackson, T.L., Grosch, C.E.: Inviscid spatial stability of a compressible mixing layer. *J. Fluid Mech.* **208**, 609–637 (1989)
15. Kudryavtsev, A.N., Khotyanovsky, D.V.: Numerical investigation of high speed free shear flow instability and Mach wave radiation. *Int. J. Aeroacoust.* **4**(3–4), 325–344 (2005)
16. Landau, L.D., Lifshitz, E.M.: Fluid Mechanics, Second Edition (Course of Theoretical Physics, Volume 6). Butterworth-Heinemann, Oxford (1987)
17. Massa, L., Austin, J.M.: Spatial linear stability analysis of a hypersonic shear layer with non-equilibrium thermochemistry. *Phys. Fluids* **20**(8), 084104 (2008)
18. Neumann von, J.: Oblique reflection of shock waves, Collected Works of J. Von Neumann, vol. 6. Pergamon Press, Oxford (1963)
19. Rikanati, A., Alon, U., Shvarts, D.: Vortex-merger statistical-mechanics model for the late time self-similar evolution of the Kelvin-Helmholtz instability. *Phys. Fluids* **15**(12), 3776–3785 (2003)
20. Rikanati, A., Sadot, O., Ben-Dor, G., Shvarts, D., Kuribayashi, T., Takayama, K.: Shock-wave Mach-reflection slip-stream instability: a secondary small-scale turbulent mixing phenomenon. *Phys. Rev. Lett.* **96**, 174503:1–174503:4 (2006)
21. Semenov, A.N., Syshchikova, M.P.: Properties of Mach reflection in shock wave intersection with a fixed wedge. *Fiz. Goren Vzryva*, No.4, pp. 596–608 (1975)
22. Semenov, A.N., Syshchikova, M.P., Berezkina, M.K.: Experimental investigation of Mach reflection in a shock tube. *Sov. Tech. Phys.* **15**, 795–803 (1970)
23. Semenov, A.N., Berezkina, M.K., Krassovskaya, I.V.: Classification of pseudo-steady shock wave reflection types. *Shock Waves* **22**, 307–316 (2012)
24. Skews, B.W.: The flow in the vicinity of a three-shock intersection. *CASI Trans.* **4**, 99–107 (1971)
25. Uskov, V.N., Chernyshov, M.V.: Special and extreme triple shock-waves configurations. *J. Appl. Mech. Tech. Phys.* **47**(4), 492–504 (2006)
26. Vasilev, E.I., Ben-Dor, G., Elperin, T., Henderson, L.F.: Wall-jetting effect in Mach reflection: Navier–Stokes Simulations. *J. Fluid Mech.* **511**, 363–379 (2004)
27. Zeldovich, Y.B.: Shock Wave Theory and Introduction to Gas Dynamics. Akademia Press, Moscow (1945). (in Russian)